Energy & Environmental Science

REVIEW

Cite this: *Energy Environ. Sci.*, 2015, **8**, 2811

Experimental demonstrations of spontaneous, solar-driven photoelectrochemical water splitting†

Joel W. Ager,*[ab] Matthew R. Shaner,[cd] Karl A. Walczak,[ab] Ian D. Sharp[ae] and Shane Ardo[f]

Received 10th February 2015,
Accepted 24th March 2015

DOI: 10.1039/c5ee00457h

www.rsc.org/ees

Laboratory demonstrations of spontaneous photoelectrochemical (PEC) solar water splitting cells are reviewed. Reported solar-to-hydrogen (STH) conversion efficiencies range from <1% to 18%. The demonstrations are categorized by the number of photovoltaic junctions employed (2 or 3), photovoltaic junction type (solid–solid or solid–liquid) and the ability of the systems to produce separated reaction product streams. Demonstrations employing two photovoltaic (PV) junctions have the highest reported efficiencies of 12.4% and 18%, which are for cells that, respectively, do and do not contain a semiconductor–liquid junction. These devices used PV components based on III–V semiconductors; recently, a number of demonstrations with >10% STH efficiency using potentially less costly materials have been reported. Device stability is a major challenge for the field, as evidenced by lifetimes of less than 24 hours in all but a few reports. No globally accepted protocol for evaluating and certifying STH efficiencies and lifetimes exists. It is our recommendation that a protocol similar to that used by the photovoltaic community be adopted so that future demonstrations of solar PEC water splitting can be compared on equal grounds.

Broader context

There is significant recent interest in solar-driven photoelectrochemical water splitting to produce hydrogen as a potential carbon-neutral transportation fuel. Renewable energy technologies must provide a positive monetary and net energy balance over their lifetimes to be viable for large scale deployment. Techno-economic analyses have suggested that solar photoelectrochemical water splitting could provide hydrogen at a cost that is competitive with energy derived from fossil fuels. Thus, economical solar water splitting represents a goal with broad-reaching appeal. One specific implementation of this concept is an integrated or monolithic solar-to-fuel conversion device that operates spontaneously, without added external electrical bias. Experimental demonstrations of such systems date back to the early 1970s, when Fujishima and Honda first reported solar water splitting using single-crystal TiO_2. This inspired considerable research in the field and to-date there have been over 40 reported demonstrations of spontaneous, solar-driven photoelectrochemical water splitting. These have led to increased fundamental and functional understanding and to increases in the overall energy-conversion efficiency. Herein, we compile reported solar-to-hydrogen conversion efficiencies and longevities. This information can be used to evaluate progress in the field and to target technical areas for future development.

[a] *Joint Center for Artificial Photosynthesis, Lawrence Berkeley National Laboratory, Berkeley, CA, USA. E-mail: JWAger@lbl.gov*
[b] *Materials Sciences Division, Lawrence Berkeley National Laboratory, Berkeley, CA, USA*
[c] *Joint Center for Artificial Photosynthesis, California Institute of Technology, Pasadena, CA, USA*
[d] *Division of Chemistry and Chemical Engineering, California Institute of Technology, Pasadena, CA, USA*
[e] *Physical Biosciences Division, Lawrence Berkeley National Laboratory, Berkeley, CA, USA*
[f] *Department of Chemistry, and Department of Chemical Engineering and Materials Science, University of California Irvine, Irvine, CA, USA*

† Electronic supplementary information (ESI) available: Additional analysis of reported STH conversion efficiency and longevity as a function of electrolyte pH and device configuration. See DOI: 10.1039/c5ee00457h

Introduction

There is considerable interest in developing technologies which could provide a sustainable alternative to the combustion of fossil fuels to meet the current and future energy demands of the planet.[1] Conversion of abundant sunlight to storable energy is an attractive approach. This concept underlies biofuel production,[2–4] as well as a number of solar-to-fuel or "artificial photosynthesis" approaches.[5–7] This review concentrates on approaches that use sunlight to split water into hydrogen and oxygen,[8] noting the recent review by Rongé *et al.*,[9] which also covers solar-driven carbon dioxide reduction. Hydrogen is a storable fuel that can be used as a feedstock for fuel cells that

generate power for transportation and, potentially, grid-scale energy storage.[10–13] Hydrogen can also be used in processes that reduce CO_2 to liquid fuels.[6]

Solar irradiation can be used for thermal and/or electrochemical water splitting.[14–17] Electrochemical water splitting requires the following overall cathodic and anodic half-reactions (in acid):[8,9]

$$2H^+ + 2e^- \rightarrow H_2 \quad (1)$$

$$H_2O \rightarrow 2e^- + 2H^+ + 1/2O_2 \quad (2)$$

The free energy change for water splitting to hydrogen (and oxygen) under standard-state conditions is $\Delta G^\circ = +237$ kJ per mol of H_2 or $\Delta E^\circ = -1.23$ V. This must be supplied by the energy in sunlight. To achieve current densities limited by the solar photon flux (~ 20 mA cm^{-2}), and considering overpotential requirements of state-of-the-art electrocatalysts and the trade-off of current and voltage in light absorbers, a total photovoltage of 1.6–1.7 V must be generated. However, the open-circuit photovoltages provided by commercially developed single-junction photovoltaic (PV) cells are typically <1 V. Therefore, either series connected cells or wide-bandgap semiconductors must be employed to drive solar water splitting in the absence of an external power source. This review article concerns experimental demonstrations of the former type. It begins with a short historical discussion of the field, which began in the peer-reviewed literature in the early 1970's with reports of photo-driven water splitting.[18,19] It focuses on trends in efficiency and stability, as well as designs of the photovoltaic and catalytic elements of the systems.

The solar-to-hydrogen (STH) conversion efficiency, η, for solar water splitting at standard temperature and pressure of H_2 and O_2 is given by:[20]

$$\eta = \frac{(1.23\ \mathrm{V})(J_{op})}{P_{in}} \quad (3)$$

where J_{op} is the operational photocurrent density in mA cm^{-2}, or the rate of hydrogen production converted to a current density, and P_{in} is the incident irradiance in mW cm^{-2}. This review describes reported STH efficiencies and stabilities because standard testing by independent research laboratories does not yet exist. The STH efficiencies are also compared to theoretical limits, and the review outlines research priorities for the field.

History of solar-driven photoelectrochemical (PEC) water splitting

In 1972, Fujishima and Honda published a report of light-driven PEC water splitting in the absence of applied electrical bias that gave rise to the modern field of artificial photosynthesis research.[18,19] Their demonstration used a single-crystal titanium oxide (TiO_2, $E_g \approx 3.0$ eV) photoanode and a platinum (Pt) cathode. Current–voltage curves were measured under illumination and oxygen was detected as a product at the photoanode. In these initial reports, product detection at the cathode and the pH of the electrolyte solution(s) contacting the electrodes were not reported. Work by other groups to reproduce the discovery established the conditions necessary for sustainable, spontaneous water splitting.[21–26]

Fujishima and Honda's report ignited considerable interest in exploring solar water splitting as a practical means to generate clean fuels and led to efforts to find other semiconductor materials that could yield higher efficiencies. Much of the subsequent work focused on wide-band gap metal oxides and oxynitrides, whose valence and conduction band positions "straddle" the water splitting redox potentials. Both powdered and electrode photocatalysts of this type have been thoroughly investigated.[27–31] However, very few of these systems achieved spontaneous (*i.e.* no applied bias) water-splitting using visible illumination and thus had very low STH conversion efficiencies. This body of work has been the subject of a number of previous recent reviews which have focused on particle photocatalyst systems.[32–40]

In 1975, Yoneyama *et al.* experimentally demonstrated that a p-GaP/n-TiO_2 tandem combination could generate H_2 and O_2 without external bias.[41] Nozik showed in 1976 that this type of tandem-junction architecture, consisting of a p-type photocathode and an n-type photoanode (Fig. 1), could achieve a higher STH conversion efficiency than a single photoelectrode.[42] Shortly after, other groups explored related tandem architectures including n-GaP/p-GaP, p-CdTe/n-TiO_2, p-CdTe/n-$SrTiO_3$, and p-GaP/n-$SrTiO_3$.[43] STH conversion efficiencies in this early work were low, $<1\%$. Also, the stability of the active components, particularly the photoanode, emerged as a critical challenge that remains to this day.[41,44,45]

Driven by advances in higher efficiency single-junction (1J) and tandem-junction (2J) solar cells in the mid-1980s, efficiencies for solar PEC water splitting also increased. For example, Bockris and co-workers reported that a p-InN photocathode wired side-by-side with an n-GaAs photoanode achieved an STH conversion efficiency of 8% and a lifetime of 10 hours.[46] Monolithic architectures using multijunction amorphous silicon (a-Si) were also explored with reported STH conversion efficiencies in the 2–3% range.[46–49]

Starting in the late 1990s high-efficiency approaches based on all III–V and Si/III–V 2J monolithic architectures were developed.

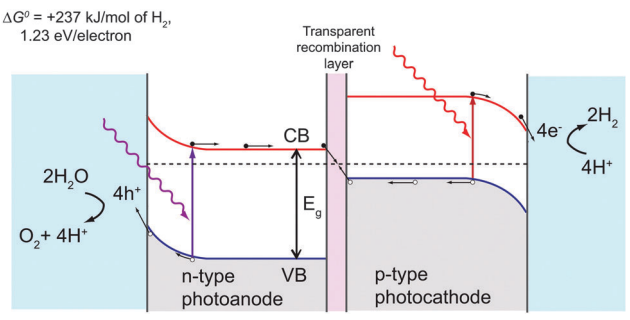

Fig. 1 Schematic of an idealized tandem-junction photoanode and photocathode device during steady-state operation. The process of solar water splitting is overlaid on the equilibrium diagram. Proton conduction in the electrolyte from the anode to the cathode is required for continuous operation. Adapted from Nozik.[42]

This work culminated in the early 2000s with demonstrations of 12 and 18% STH conversion efficiencies by Turner and co-workers and by Licht *et al.*, respectively.[50–52] Triple-junction (3J) amorphous silicon (a-Si) cells were also investigated starting in the late 1980s, as their open-circuit photovoltage can exceed 2 V.[50,53–56] Miller and co-workers reported STH conversion efficiencies as high as 8% with this approach.[50,56] It is also notable that the longest reported operational stability for solar-driven PEC water splitting, more than a month, was achieved by Kelly and Gibson with this architecture.[49]

Since 2010, there have been significant efforts to replace noble-metal electrocatalysts with those made from less expensive elements, to use metal-oxide light absorbers that may be more stable, and to demonstrate fully integrated devices (*i.e.*, those with intimate contact between all light absorbing and catalytic components without wires). The first fully integrated demonstration was in 2011 by Nocera and co-workers where an STH conversion efficiency of 2.5% was reported for a *completely integrated* 3J a-Si cell incorporating hydrogen and oxygen evolution catalysts made from abundant elements on its surfaces.[57] A number of notable recent reports use metal oxide absorbers such as WO_3, Fe_2O_3, and $BiVO_4$. By coupling with dye sensitized solar cells and 1J and 2J a-Si solar cells, STH efficiencies ranging from 2% to over 5% have been achieved.[58–60]

While systems of integrated photovoltaic and catalytic components may be conceptually attractive, physically separating the photovoltaic (PV) and electrocatalyst materials can circumvent some of the stability issues that are present in the more integrated PEC water splitting demonstrations. Four recent reports that demonstrate this approach include: 15% STH conversion efficiency using three side-by-side 3J III–V/Ge cells with 10× optical concentration,[61] 10% STH conversion efficiency using three series-connected, side-by-side $CuIn_xGa_{1-x}Se_2$ (CIGS) solar cells,[62] 12% STH conversion efficiency using two organic–inorganic halide perovskite solar cells,[63] and 10% STH conversion efficiency using 4 side-by-side Si minimodules.[64]

Very recently, since 2013, efforts to use non-planar semiconductor geometries and advanced photon management strategies and concepts have received interest. These approaches have a number of potential advantages. The directions of light absorption and charge separation can be orthogonalized, allowing the use of less pure materials,[65] and properly designed arrays can use light trapping to reduce the amount of required absorber material.[66] There are a few reports of achieving spontaneous solar-driven water splitting using this type of approach but, so far, the reported STH efficiencies have remained low (<1%).[67–69]

Nomenclature, device description, and data presentation

Device description. The nomenclature used herein is adopted from a recent photoelectrochemical taxonomy, which is summarized in Table 1.[70] All electrical architectures covered in this review consist of two or three photovoltaic junctions connected electrically in series. Unless otherwise noted, the optical architecture is assumed to be a stacked arrangement, with the higher bandgap absorber on top, facing the light source. Side-by-side arrangements are also reported and are designated as such. We also distinguish between integrated cells and those in which wires connect the PV cells.

We make a distinction between cells that use semiconductor–liquid junctions to separate photoinduced charge carriers, as shown in Fig. 1, with those that use ''buried'' solid–solid junctions (*e.g.* pn) to perform the charge separation. Devices that use at least one semiconductor–liquid junction are called ''photoelectrosynthetic'' and those that employ buried junctions are called ''photovoltaic-biased electrosynthetic.'' We also denote the method used to electrically connect the PV junction to the HER and OER catalysts, if these are employed in the design. In integrated devices, the catalysts are directly deposited on the PV element, often as a thin film or as nanoparticles. In other approaches, the catalyst is wired to the PV element(s). Approaches that wire both the HER and OER catalysts are often called ''PV + electrolyzer.'' Finally, we note whether or not the demonstration attempted to separate the chemical reaction products to yield a

Table 1 Device nomenclature

SLJ	Semiconductor–liquid junction
Photoelectrosynthetic cell	A cell whose photo-voltage producing junctions are all semiconductor–liquid in character
Photovoltaic-biased photoelectrosynthetic cell	A cell whose photo-voltage producing junctions consist of at least one semiconductor–liquid junction and one solid-state junction
Photovoltaic-biased electrosynthetic cell	A cell whose photo-voltage producing junctions are all solid-state in character
Tandem junction (2J)	A device containing two photo-voltage producing junctions
Triple junction (3J)	A device containing three photo-voltage producing junctions
a	Amorphous
c	Crystalline
Pin	Buried junctions in series as p-type, intrinsic, and then n-type
DSSC	Dye-sensitized solar cell
CIGS	$CuIn_xGa_{1-x}Se_2$
OER	Oxygen-evolution reaction
HER	Hydrogen-evolution reaction
PEM	Proton-exchange membrane
MEA	Membrane-electrode assembly
Photocatalyst	A single material that simultaneously acts as semiconductor light absorber and as catalyst
Co-evolved products	H_2 and O_2 evolve without a physical barrier such as a membrane or separator to prevent chemical cross-over
Integrated	Intimate contact between the catalyst and semiconductor surface
Wired	Physically separated catalyst and semiconductor surfaces connected through a wire or the equivalent

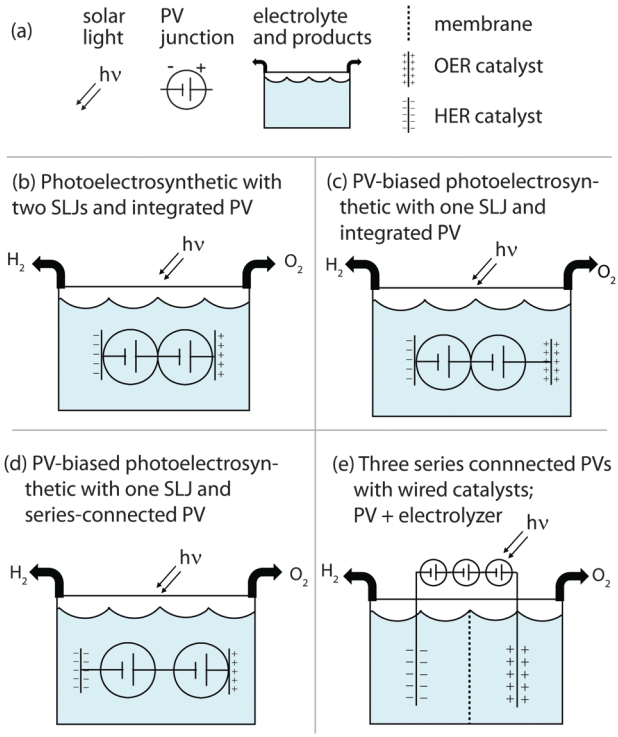

Fig. 2 Depiction of commonly employed solar photoelectrochemical water splitting architectures in circuit diagram form. (a) Key for symbols used; see Table 1 for abbreviations. Wires are indicated by solid lines. If elements are touching without a wire (*e.g.* the PVs) they are monolithically integrated. (b) The photoelectrosynthetic geometry shown in Fig. 1 with integrated PV elements and with both catalysts integrated. (c) A PV-biased photoelectrosynthetic device with one buried junction (the photoanode wired to the OER catalyst) and one SLJ. (d) A PV-biased photoelectrosynthetic device with series-connected PV elements where the OER catalyst is integrated and the HER catalyst is wired. (e) A PV + electrolyzer approach with 3 PV cells wired in series and a membrane is used to separate chemical reaction products.

pure H_2 fuel stream. Fig. 2 depicts some of the more commonly employed geometries in the form of circuit diagrams.

Device performance. The data summarized in the tables and figures that follow are reported directly from the original references. The only change which has been made is correction of efficiencies reported using the higher heating value of H_2 (1.48 eV per electron); in these cases, the efficiencies were adjusted to use the free energy of the water splitting reaction (1.23 eV per electron).[71]

There are a number of published recommendations for standardized photoelectrochemical testing of half cells and full cells.[71–73] Ideally, analogous with the well-established testing protocols for solar cells,[74] the STH efficiency of each demonstration would be confirmed by an independent testing laboratory using incident light that corresponds to the solar spectrum, together with direct and accurate measurement of H_2 and O_2 products. However, independent testing labs of this type do not currently exist for solar PEC water splitting or for any other solar-to-fuel conversion technology.

Thus, most of the demonstrations used solar simulators optimized for testing Si solar cells and calculated the STH conversion efficiency *via* a current density measurement assuming 100% Faradaic efficiency for H_2 production. Accurate testing of tandem solar cells, the type of architecture used by most of the demonstrations in this review, actually requires careful control of temperature, solar simulator spectrum, and a number of other factors.[75] Also, most of the studies measured the current only; quantification of the amount of H_2 and O_2 generated, and confirmation of their 2 : 1 ratio expected from reactions (1) and (2), was less common.

A consensus definition of device stability that is evaluated by most researchers does not yet exist in the solar PEC water splitting community. In this review, we tabulate, if available, the duration and results of long-term testing performed on the devices. We also note, briefly, the criterion used by the authors to evaluate or terminate their stability test. Most often, the authors either establish a period of time over which the photocurrent is reasonably stable or, alternatively, drops by *ca.* 10–20%. Less common is the monitoring of H_2 (and even less commonly, O_2) over time. We also observe that, in the vast majority of cases, stability data from a single device is presented. This contrasts with the parallel testing, often under accelerated conditions, which is used in the evaluation of PV device lifetimes.

In the absence of accepted standards and independent testing, it is not valid to directly compare the claimed STH efficiencies and stabilities reported herein or to declare a "world record." Nevertheless, the two tabulated metrics (STH conversion efficiency and device stability) currently provide a means of tracking progress and identifying bottlenecks in the field. Finally, it is important to acknowledge that achieving ultimate efficiency or stability was not necessarily the primary objective for many of the reports of solar water splitting. Instead, much of the work was dedicated to exploring new approaches or concepts in photoelectrochemical energy-conversion research.

Data presentation and guide to tables. Experimental reports of spontaneous solar water splitting are summarized in Fig. 3, with the reported STH conversion efficiency graphed *versus* the year of the report. Tables 2–5 contain short descriptions of the demonstrations presented in reverse chronological order. Fig. 3 is analogous to the plot of solar PV efficiency *versus* time maintained by the National Renewable Energy Laboratory[76] and the tables are modelled after a semi-annual report of "world records" and "notable exceptions" for PV solar cells.[74] The tables are grouped by the number and type of PV junction(s) as follows:

Table 2: 2J PEC cells with at least one SLJ,

Table 3: 2J PV-biased electrosynthetic cells, including PV + electrolyzer approaches.

Table 4: 3J PEC cells with at least one SLJ, and

Table 5: 3J PV-biased electrosynthetic cells including PV + electrolyzers.

The format used for each entry is as follows.

Photocathode//photoanode

Architecture and/or configuration

Configuration and type of HER catalyst

Configuration and type of OER catalyst

For example, the following description,

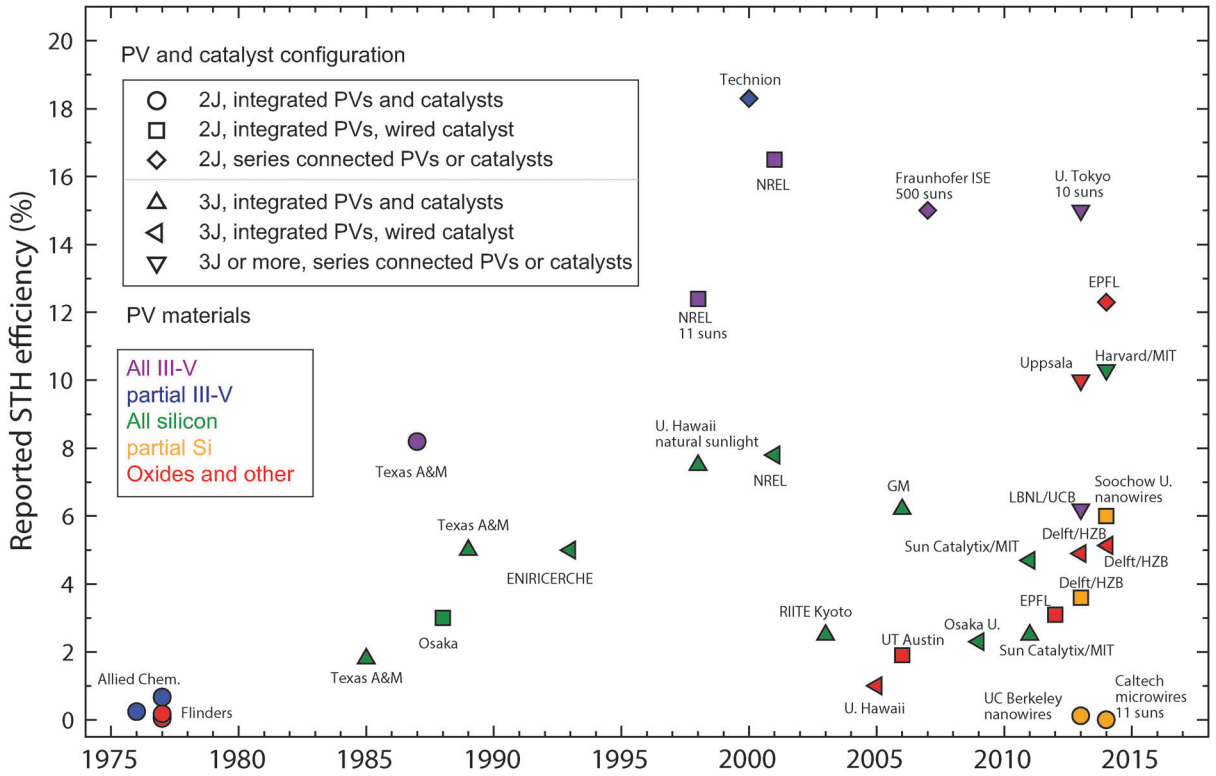

Fig. 3 Reported solar to hydrogen (STH) conversion efficiencies as a function of year and sorted by the number of tandem photovoltaic junctions used (2 or 3). The degree of integration of photovoltaic and catalyst elements is also distinguished, see Fig. 2. The fill colour represents the semiconductor materials used in the photovoltaic portion of the device. All STH conversion efficiencies are as reported in the original publications (see Tables 2–5).

$GaInP_2$(pn)//GaAs(pn)
monolithic PV
wired Pt cathode
integrated Pt OER catalyst,

is for a GaInP–GaAs monolithic tandem solar cell with buried pn junctions for both the 1.8 eV bandgap top cell and 1.4 eV bandgap bottom cell.[50] H_2 production is at a remote Pt cathode wired to the GaInP cathode. O_2 production occurs at the surface of the GaAs, which is coated by Pt.

Discussion

Solar-to-hydrogen conversion efficiency

It is interesting to compare the reported efficiencies to calculations of the theoretical limits for tandem solar to hydrogen conversion.[94–100] While the assumptions regarding catalyst overpotentials and device architectures vary, the consensus of these studies is that a STH conversion efficiency of >25% is possible with a 2J approach for integrated systems in which the catalyst and absorber areas are equivalent. Both 1J and 3J approaches have lower efficiency limits. For 1J devices, the absorber bandgap necessary to generate the required voltage (1.6–1.7 V) at the point of maximum power generation significantly limits the usable solar photon energies and thus results in current densities below those for 2J devices. 3J devices have the highest demonstrated efficiencies for PV power generation (for both 1 sun and optical concentration conditions), but this is the result of a relatively high photovoltage and low photocurrent density at the point of maximum power generation. However, if the absorber junction area and catalyst surface area can be independently varied to optimize the photovoltaic power curve to the catalyst load curve, as in the PV + electrolyzer approaches, higher efficiencies are possible with three or more junctions.[61,101] It is clear from Fig. 3 that the experimentally demonstrated STH efficiencies to date (<19%) are far from the theoretical limit. This contrasts somewhat with the situation for solar photovoltaics, where recent work has produced single-junction cells close to the theoretical limit (*e.g.* GaAs with near 30% efficiency compared to the thermodynamic limit of ~31%).[74,102,103]

Architectures and semiconductor–liquid *vs.* solid state junctions

Subject to the constraints discussed above regarding direct comparison of STH efficiency values, it is nevertheless interesting to compare the approaches used to achieve relatively high STH conversion efficiencies. There are 8 reports of >10% efficiency depicted in Fig. 3. Six of these can be categorized as photovoltaic-biased electrosynthetic, or "PV + electrolyzer", approaches with essentially decoupled PV and catalytic functions.[52,61–64,84] The remaining two demonstrations are from Turner and co-workers.[50,51] One of these employed two buried PV junctions in $GaInP_2$ and GaAs with a wired Pt cathode and an integrated Pt anode. The other device, the so-called

Table 2 Two junction (2J) tandem PEC cell water-splitting demonstrations with at least one semiconductor–liquid junction (SLJ) listed in reverse chronological order. The best-in-class efficiency is displayed in bold typeface and the best-in-class stability is italicized

Publication institute(s)	Device structure (cathode//anode)	Electrolyte and illumination conditions	STH efficiency	Stability, notes
Bornoz *et al.*[77] (2014) EPFL, Institute for Solar Fuels, Delft University	SLJ Cu_2O(p)//$BiVO_4$(n) SLJ wired PV integrated RuO_x HER catalyst integrated CoP_i OER catalyst	$K_{3-x}H_xPO_4$ buffer, pH 6 co-evolved products 100 mW cm^{-2}	0.5%	2 minutes 20% current loss
Wang *et al.*[78] (2014) Beijing Normal University, Chinese Academy of Sciences, Soochow University	c-Si(pn)//Fe_2O_3(n) SLJ core–shell nanowire monolithic PV wired Pt HER catalyst integrated Au OER catalyst	1 M Na_3PO_4 co-evolved products 60 mW cm^{-2}	6.0%	40 minutes measurement of O_2
Shaner *et al.*[68] (2014) Caltech, JCAP	c-Si(pn)//WO_3(n) SLJ core–shell nanowire monolithic PV wired Pt cathode	1 M H_2SO_4 co-evolved products 1080 mW cm^{-2} (~11 suns)	0.0068%	10 min stable current
Liu *et al.*[67] (2013) UC Berkeley	c-Si(pn)//TiO_2(n) SLJ core–shell nanowire monolithic PV integrated Pt HER catalyst integrated IrO_x OER catalyst	0.5 M H_2SO_4 co-evolved products 150 mW cm^{-2} (1.5 suns)	0.12%	4.5 hours H_2 and O_2 generation rate measured
Abdi *et al.*[59] (2013) Delft University, HZB Berlin	a-Si:H(pin)//$BiVO_4$(n) SLJ wired Pt HER catalyst integrated CoP_i OER catalyst	pH 7.3 co-evolved products 100 mW cm^{-2}	3.6%	1 hour stable current
Brillet *et al.*[58] (2012) EPFL	DSSC//WO_3(n) SLJ DSSC//Fe_2O_3(n) SLJ wired PV wired Pt HER catalyst integrated Al_2O_3,Co OER catalyst	1 M $HClO_4$, pH 0, 1 M NaOH, pH 13.6, respectively co-evolved products 100 mW cm^{-2}	3.1%, 1.17%, respectively	8 hours 30% current drop
Lin *et al.*[79] (2012) University of Cambridge	SLJ Cu_2O//WO_3(n) SLJ wired PV integrated NiO_x HER catalyst	0.1 M Na_2SO_4, pH 6 100 mW cm^{-2}	0.04%	Not reported
Park and Bard[80] (2006) UT Austin	DSSC//WO_3(n) SLJ wired PV wired Pt HER catalyst	0.25 M Na_2SO_4, pH 4 200 mW cm^{-2}	1.9%	30 min measurement of H_2
Khaselev and Turner*[51] *(1998) ***NREL***	***SLJ $GaInP_2$(p)//GaAs(pn)*** ***monolithic PV*** ***integrated Pt HER catalyst*** ***wired Pt OER catalyst***	***3 M H_2SO_4,*** ***0.01 M triton X-100*** ***co-evolved products*** ***11 suns***	***12.4%***	***20 hours*** ***20% drop in current***
Kainthla *et al.*[46] (1987) Texas A&M	SLJ InP(p)//GaAs(n) SLJ cells wired side-by-side integrated Pt HER catalyst integrated MnO OER catalyst	6 M KOH	8.2%	10 hours initial 10% current drop

Table 2 (*continued*)

Publication institute(s)	Device structure (cathode//anode)	Electrolyte and illumination conditions	STH efficiency	Stability, notes
Nakato *et al.*[81] (1982) Osaka University	CdS(n)//TiO_2(n) SLJ wired PVs wired Pt cathode	1.0 M NaOH co-evolved products 250 W Hg lamp	Not reported	1 hour steady photocurrent
Mettee *et al.*[82] (1981) UC Berkeley	SLJ GaP(p)//Fe_2O_3(n) SLJ wired PV integrated Pt HER catalyst integrated RuO_2 OER catalyst	1 M Na_2SO_4 fritted compartments sunlight	0.02–0.1%	Not reported
Ohashi *et al.*[43] (1977) Flinders University, Adelaide, South Australia	SLJ CdTe(p)//TiO_2(n) SLJ SLJ GaP(p)//TiO_2(n) SLJ SLJ CdTe(p)//SrTiO3(n) SLJ SLJ GaP(p)//$SrTiO_3$(n) SLJ cells wired side-by-side	1 M NaOH co-evolved products 100 mW cm^{-2}	0.044%, 0.098%, 0.18%, 0.67%, respectively	1 hour stable photovoltage some cells tested to 50 hours
Morisaki *et al.*[83] (1976) University of Electro-Communications	c-Si(pn)//TiO_2(n) SLJ monolithic PV wired Pt cathode	0.1 M NaOH co-evolved products sunlight	0.1%	Not reported
Nozik[42] (1976) Materials Research Center, Allied Chemicals Corp.	SLJ GaP(p)//TiO_2(n) SLJ wired PVs	0.2 N H_2SO_4 co-evolved products 85 mW cm^{-2}	0.25%	Not reported

"Turner cell", uses a semiconductor–liquid junction for the photocathode. To date, no other semiconductor–liquid junction devices have been able to approach the Turner cell's efficiency of 12.4%.[51] The challenges responsible for the low SLJ device efficiencies are the availability of combinations of stable photocathode and photoanode materials with bandgaps commensurate with the solar spectrum and optimized band-edge positions for the hydrogen and oxygen evolution reactions. Solutions to these challenges, including new material discoveries, will be required for SLJ devices to rival non-SLJ device efficiencies.

Semiconductor materials

Traditionally, semiconductor materials used in the high efficiency PEC devices have been first developed by the solid-state photovoltaics community and adapted for use in PEC cells. The first demonstrations to claim >10% STH conversion efficiency utilized Si and compound III–V and II–VI materials (purple and blue points in Fig. 3).[50–52,84] More recently, materials such as CIGS and halide perovskite-based cells have been adapted into PEC cells that exceeded 10% STH efficiency.[62–64] Over the last decade, materials such as metal oxides, which have been developed specifically for PEC applications, have seen substantial research interest and progress. Reported STH efficiencies for devices containing metal-oxide-based active components now exceed 5%.[60]

Optical concentration

Optical concentration has also been used in some of the >10% efficient devices depicted in Fig. 3 because it can enhance photovoltaic efficiencies and utilize smaller areas of semiconductor material.[51,84,101] Furthermore, concentrator configurations have the potential to reduce the volume of electrolyte and the balance of systems burdens associated with liquid handling. However, additional engineering challenges arise from optical concentration in integrated PEC devices because the increased current density may increase the load on the catalyst and introduce ionic conduction limitations in solution, depending on the specific design. In addition, optical concentration results in increased photovoltage, which is desired, and increased temperature, which is detrimental for photovoltaic performance but beneficial for increasing catalytic activity. The complex trade-offs between these phenomena have been subject of recent investigations,[97] and deserve more attention toward development of efficient designs.

Stability

Device stability is a critical challenge for PEC devices to be commercially deployable. Renewable energy technologies must provide a positive monetary and net energy balance over their lifetimes to be viable for large scale deployment. Studies which have considered the techno-economic[104,105] and energy balance[106,107] considerations of practical PEC solar to hydrogen conversion have recommended minimum operational lifetimes of at least several years as well as efficiencies exceeding 10%.

Table 3 Two junction (2J) photovoltaic-biased electrosynthetic cell (including PV + electrolyzer) demonstrations of solar water splitting in reverse chronological order. The best-in-class reported efficiency is displayed in bold typeface and the best-in-class reported stability is italicized

Publication institute(s)	Device structure	Electrolyte and illumination conditions	STH efficiency	Stability
Luo *et al.*[63] (2014) EPFL	Halide perovskite ($CH_3NH_3PbI_3$) 2 cells wired side-by-side wired NiFe HER catalyst wired NiFe OER catalyst PV + electrolyzer	1 M NaOH Co-evolved products 100 mW cm^{-2}	12.3%	2 hours stable photocurrent and H_2/O_2 production 10 hours small degradation
Peharz *et al.*[84] (2007) ISE Fraunhofer, Freiburg, Germany	$Ga_{0.83}In_{0.17}As(pn)//Ga_{0.35}In_{0.65}P(pn)$ monolithic PV wired Pt HER catalyst wired IrO_2 OER catalyst Nafion MEA PV + electrolyzer	pH 7 membrane separated evolution of products 500× optical concentration	15%[a]	2.3 hours stable current in outdoor test
Khaselev *et al.*[50] (2001) NREL	$GaInP_2(pn)//GaAs(pn)$ monolithic PV wired Pt HER catalyst integrated Pt OER catalyst	2 M KOH co-evolved products 100 mW cm^{-2}	16.5%	9 hours stable current in outdoor test
***Licht et al.*[52] (2000) Technion, Israel**	***$Al_{0.15}Ga_{0.85}As(pn)//Si(pn)$ monolithic PV integrated Pt HER catalyst integrated RuO_2 OER catalyst PV is not in contact with electrolyte***	***1 M $HClO_4$ co-evolved products 135 mW cm^{-2}***	***18.3%***	***14 hours stable photocurrent***
Sakai *et al.*[48] (1988) Osaka University	a-Si(pin)//a-Si(pin) monolithic PV integrated Pt HER catalyst wired RuO_2 OER catalyst	0.5 M H_2SO_4 co-evolved products 100 mW cm^{-2}	2.93% a-Si in solution 3.23% a-Si out of solution	Not reported

[a] Value adjusted from that reported using higher heating value of H_2. Reported value is that obtained after multiplication by (1.23/1.48).

Table 4 Triple junction (3J) tandem PEC cell water-splitting demonstrations with at least one semiconductor–liquid junction (SLJ) listed in reverse chronological order. The best-in-class reported efficiency is displayed in bold typeface and the best-in-class reported stability is italicized

Publication institute(s)	Device structure	Electrolyte and illuminationconditions	STH efficiency (%)	Stability, notes
Walczak et al.[85] *(2015)* *LBNL, Caltech, JCAP*	*c-Si(pn^+)//c-Si(p^+n)//WO_3 SLJ* *monolithic PV* *Integrated Pt HER catalyst with TiO_2 passivation layer*	*1 M $HClO_4$* *Membrane Nafion XL* *200 mW cm^{-2}*	*0.24*	*20 hours* *stable H_2 generation* *tested to 48 hours*
Han *et al.*[60] (2014) **Delft University, HZB Berlin**	**a-Si:H(pin)//nc-Si:H(pin)//$BiVO_4$(n) SLJ** **micromorph Si monolithic** **wired Pt HER catalyst** **integrated CoPi OER catalyst**	**pH 7** **co-evolved products** **100 mW cm**	5.2	**1 hour** **<5% current loss**
Abdi *et al.*[59] (2013) Delft University, HZB Berlin	a-Si:H(pin)//a-Si:H(pin)//$BiVO_4$(n) SLJ a-Si monolithic wired Pt HER catalyst integrated CoPi OER catalyst	pH 7.3 co-evolved products 100 mW cm^{-2}	4.9	1 hour stable photocurrent
Gaillard *et al.*[86] (2010) U. Hawaii	a-Si(pin)//a-Si(pin)//WO_3(n) SLJ monolithic PV wired Pt HER catalyst	0.33 M H_3PO_4 co-evolved products 100 mW cm^{-2}	3.0	Not reported
Zhu *et al.*[87] (2010) U. Hawaii, MV Systems, NREL	SLJ a-SiC:H(ip)//a-Si(pin)//a-Si(pin) monolithic PV wired RuO_2 OER catalyst	pH 2 sulphamic acid solution with added potassium biphthalate co-evolved products	1.6	Not reported for integrated device
Brillet *et al.*[88] (2010) EPFL	DSSC//DSSC//Fe_2O_3(n) SLJ wired PV wired Pt HER catalyst	1 M NaOH, pH 13.6 co-evolved products 100 mW cm^{-2}	1.36	Not reported
Miller *et al.*[89] (2005) U. Hawaii	a-Si(pin)//a-Si(pin)//WO_3(n) SLJ monolithic PV wired Pt HER catalyst	1 N H_3PO_4 co-evolved products 100 mW cm^{-2}	0.7	10 hours stable H_2 production

Table 5 Triple junction photovoltaic-biased electrosynthetic cell (PV + electrolyzer) demonstrations of solar water splitting in reverse chronological order. The best-in-class reported efficiency is displayed in bold typeface, and best-in-class reported stability is italicized. Approaches using 4 junctions are also included here

Publicationinstitute(s)	Device structure	Electrolyte and illumination conditions	STHefficiency	Stability, notes
Cox *et al.*[64] (2014) Harvard and MIT	Si minimodule 4 modules side by side wired NiMoZn HER catalyst wired NiB OER catalyst	pH 9.2 100 mW cm^{-2}	9.7% current and H_2 and O_2 production measured	168 hours constant current density
Modestino *et al.*[90] (2014) UC Berkeley and LBNL	$GaInP_2$(pn)/GaAs(pn)/Ge(pn) 3J monolithic PV wired Pt HER catalyst wired Pt OER catalyst	pH 9.2 nafion membrane and electrolyte recirculation 100 mW cm^{-2}	6.2% current and H_2 production measured	15 hours constant current density
Jacobsson *et al.*[62] (2013) Uppsala University	$CuIn_xGa_{1-x}Se_2$(pn) 3 cells wired side-by-side wired Pt HER catalyst wired Pt OER catalyst	3 M H_2SO_4 co-evolved products 100 mW cm^{-2}	10%	27 hour stable H_2 productions
Fujii *et al.*[61] (2013) **U. Tokyo**	**GaInP(pn)/InGaAs(pn)/Ge(pn) 3J** **wired Pt HER catalyst** **wired Pt OER catalyst** **nafion MEA**	**pH 7** **10× optical concentration**	**15% (3 solar cells, two PEM electrolyzers), 12% (one PV, one PEM)**	**1 hour** **constant current and H_2 production**
Reece *et al.*[57] (2011) Sun Catalytix, MIT	a-Si(pin)//a-Si(pin)//a-Si(pin) monolithic PV integrated NiMoZn HER catalyst integrated Co OER catalyst	pH 9.2 co-evolved products 100 mW cm^{-2}	4.7% wired, 2.5% integrated cathode	24 hours 20% drop in O_2 production
Yamane *et al.*[91] (2009) Osaka University, Gifu University, CREST	c-Si(n)–CuI(p)//a-Si(pin)//GaP(pn) wired Pt HER catalyst integrated RuO_2 OER catalyst	0.1 M Na_2SO_4 (pH 6.3) co-evolved products 100 mW cm^{-2}	2.3%	3 hours constant current
Kelly and Gibson[49](2006) *General Motors*	*a-Si(pin)//a-Si(pin)//a-Si(pin) monolithic PV* *wired Pt or Ni HER catalyst* *integrated FTO OER catalyst*	*5 M KOH* *co-evolved products* *100 mW cm^{-2}*	*6.2%*	*31 days* *stable current density*
Park and Bard[92] (2005) UT Austin	DSSC//DSSC//DSSC 3 cells wired side by side wired Pt HER catalyst integrated Pt OER catalyst	2 M KOH KOH salt bridge 100 mW cm^{-2}	3.7%	20 hours stable current density
Yamada *et al.*[93] (2003) Research Institute of Innovative Technology for the Earth, Kyoto, Japan	a-Si(pin)//a-Si(pin)//a-Si(pin) monolithic PV integrated Co–Mo HER catalyst integrated Ni–Fe–O OER catalyst	pH 13 co-evolved products 100 mW cm^{-2}	2.5%	18 hours 10% drop in current density (<1 hour@pH 14)
Khaselev *et al.*[50] (2001) NREL	a-Si(pin)//a-Si(pin)//a-Si(pin) monolithic PV integrated Pt HER catalyst wired Pt OER catalyst	2 M KOH co-evolved products 100 mW cm^{-2}	7.8%	Not reported
Rocheleau *et al.*[56] (1998) U. Hawaii	a-Si(pin)//a-Si(pin)//a-Si(pin) monolithic PV integrated $Co_{0.73}Mo_{0.27}$ HER catalyst integrated $NiFe_{0.19}O_{2.2}$ OER catalyst	1 N KOH co-evolved products natural sunlight	7.5%	2 hours stable current in outdoor test

Table 5 (*continued*)

Publication institute(s)	Device structure	Electrolyte and illumination conditions	STH efficiency	Stability, notes
Gramaccioni *et al.*[55] (1993) ENIRICERCHE, Rome, Italy	a-Si(pin)//a-Si(pin)//a-Si(pin) monolithic PV integrated Pt HER catalyst wired RuO_2 OER catalyst	0.5 N H_2SO_4 co-evolved products 100 mW cm^{-2}	~5%	Not reported
Lin *et al.*[54] (1989) Texas A&M	a-Si(pin)//a-Si(pin)//a-Si(pin) monolithic PV integrated Pt HER catalyst integrated RuO_2 OER catalyst	1 M H_2SO_4 co-evolved products 100 mW cm^{-2}	5%	6 hours STH > 4%
Delahoy *et al.*[53] (1985) Texas A&M	a-Si(pin)//a-Si(pin)//a-Si(pin) monolithic PV integrated Pt HER catalyst integrated RuO_2 OER catalyst	5 M H_2SO_4 co-evolved products 100 mW cm^{-2}	1.8%	Not reported

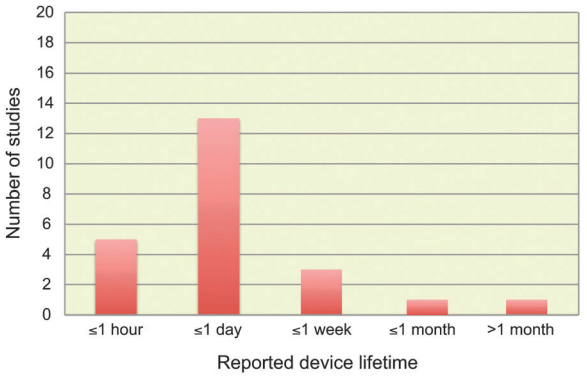

Fig. 4 Histogram of reported lifetimes for the overall water splitting devices tabulated in Tables 2–5. Long-term operational stability remains a central challenge for achieving scalable systems.

Fig. 4 summarizes the reported stability lifetimes for all devices in Tables 2–5. Typically, stability was assessed by monitoring the current density as a function of time under constant illumination. More functionally relevant testing, such as continuous measurement of H_2 and O_2 production, light–dark cycling, variation of temperature, and/or accelerated wear has not typically been employed. Most reports assessed stability of 24 hours or less. It can also be observed that the majority of devices with longer lifetimes consisted of photovoltaic cells isolated from the electrolyte.[49,62,84] Only a few SLJ devices have reported stabilities of >1 day.[87] Additional information regarding longevity is provided in the ESI.†

Long term stability presents considerable challenges for the materials in contact with the electrolyte. Only a few materials, such as TiO_2 and $SrTiO_3$, are thermodynamically stable under conditions relevant to solar PEC water splitting.[45,108] Accordingly, some recent efforts toward increasing device longevity have focused on the passivation of photoelectrodes through application of optically transparent and electronically conductive metal and/or metal-oxide coatings by atomic layer deposition (ALD) or physical vapor deposition (PVD). This was recently reviewed by Liu *et al.*[109]

Solar fuels production

The vast majority of the studies complied in this report either co-generated H_2 and O_2 or generated them in separated cathode and anode chambers. In a practical solar to H_2 generating device, separation of products will eventually be required to prevent gas crossover, prevent the formation of explosive mixtures, and ultimately yield a pure stream of H_2 fuel. Of the work reviewed here, only a few studies have used a separator, ion-conducting membrane, or equivalent to affect product separation.[61,84,90,101] This aspect of solar PEC hydrogen production is relatively underdeveloped, but is important in the design and development of deployable devices.[110]

Finally, we comment briefly on the eventual economic viability of solar-driven PEC water splitting. Ultimately, the cost of the H_2 fuel produced by the process should be cost competitive with fossil fuels. A full discussion of this topic is beyond

the scope of this review; we refer the reader instead to the recent techno-economic analyses of Pinaud *et al.*[105] and Rodriguez *et al.*[110] which have analysed and discussed prospective solar H_2 generation costs. However, it is interesting to compare the cell-level efficiency and longevity data compiled in this review to published technology targets. For example, the US DOE Hydrogen Production Program (Fuel Cell Technologies Office (FCTO), Office of Energy Efficiency and Renewable Energy (EERE)) maintains a road map for solar PEC water splitting. The STH efficiency and cost targets, for $\geq$98% purity H_2 at 300 psig at the plant gate, are 15% STH and \$17.30 per kg H_2 by 2015, 20% STH and \$5.70 per kg H_2 by 2020, and ultimately 25% STH and \$2.10 per kg H_2.[111] No laboratory-scale devices meet the 2020 STH target, although there are some demonstrations meeting the 2015 STH efficiency target of 15%.[50,61,84,96] However, the III–V materials used in those demonstrations are likely not compatible with the cost targets. Significant progress in the application of low-cost materials deposited using methods compatible with large-scale manufacturing to high-efficiency water splitting will be required to meet these technology goals.

Conclusions

Experimental demonstrations of photoelectrochemically driven water splitting using solar light are reviewed. The review includes devices that operate spontaneously, without additional applied bias, and those that used a tandem photovoltaic approach to provide the electrical driving force. Over 40 studies dating from the early 1970s to the present are included. Reported solar to hydrogen conversion efficiencies are compiled, though it is noted that these values have some uncertainty due to the lack of a standardized and independent testing procedure.

Reported solar to hydrogen conversion efficiencies vary from $<$1% up to 18%; however, only a few studies report a value of $>$10%. These demonstrated efficiencies are far lower than predicted theoretical efficiency limits of $>$25% which could be achieved with ideal semiconductors and catalysts. Of the reports of $>$10% STH efficiency, most used III–V semiconductors for their photovoltaic elements, but we note recent progress in the application of potentially less costly materials such as Si, CIGS, and halide perovskites.

Reported device longevity is also compiled. Most devices are reported to function for a day or less and there are very few demonstrations of longer operation. Improvements in this area, as well as the need for accelerated wear testing, are identified as critical research needs. Recent techno-economic and life cycle assessments of solar water systems have identified STH efficiency and longevity as the primary factors contributing to positive energy return on energy invested. Achieving the combination of efficiency and longevity needed for technological advancement will require basic and applied research breakthroughs in improving device stability, determining and eliminating of photocarrier recombination and voltage loss mechanisms, and engineering design of simultaneously low-loss and operationally safe complete systems.

Acknowledgements

The authors thank Dr Eric Miller for the inspiration to compile this review, and the members of the U.S. Department of Energy's Photoelectrochemical Working Group and Task 35 (Renewable Hydrogen) of the International Energy Agency's Hydrogen Implementing Agreement for helpful comments, suggestions, and discussions, especially Heli Wang, Keith Emery, and Tom Jaramillo. JWA, KAW, IDS, and MS were supported by the Joint Center for Artificial Photosynthesis, a DOE Energy Innovation Hub, supported through the Office of Science of the U.S. Department of Energy under Award Number DE-SC0004993. SA acknowledges support from the Department of Chemistry and the School of Physical Sciences at the University of California, Irvine. MS acknowledges the Resnick Institute for Sustainability for a graduate fellowship. A summary version of this review paper (DOI: 10.2172/1209500) can be found on the working group website http://energy.gov/eere/fuelcells/photoelectrochemicalworking-group). The STH efficiency tables and graph will be updated as the field progresses.

References

1 S. Chu and A. Majumdar, *Nature*, 2012, **488**, 294–303.
2 E. D. Larson, *Energy Sustainable Dev.*, 2006, **10**, 109–126.
3 J. J. Cheng and G. R. Timilsina, *Renewable Energy*, 2011, **36**, 3541–3549.
4 R. E. Blankenship, D. M. Tiede, J. Barber, G. W. Brudvig, G. Fleming, M. Ghirardi, M. R. Gunner, W. Junge, D. M. Kramer, A. Melis, T. A. Moore, C. C. Moser, D. G. Nocera, A. J. Nozik, D. R. Ort, W. W. Parson, R. C. Prince and R. T. Sayre, *Science*, 2011, **332**, 805–809.
5 J. A. Turner, *Science*, 2004, **305**, 972–974.
6 C. Graves, S. D. Ebbesen, M. Mogensen and K. S. Lackner, *Renewable Sustainable Energy Rev.*, 2011, **15**, 1–23.
7 D. G. Nocera, *Acc. Chem. Res.*, 2012, **45**, 767–776.
8 M. G. Walter, E. L. Warren, J. R. McKone, S. W. Boettcher, Q. X. Mi, E. A. Santori and N. S. Lewis, *Chem. Rev.*, 2010, **110**, 6446–6473.
9 J. Rongé, T. Bosserez, D. Martel, C. Nervi, L. Boarino, F. Taulelle, G. Decher, S. Bordiga and J. A. Martens, *Chem. Soc. Rev.*, 2014, **43**, 7963–7981.
10 P. P. Edwards, V. L. Kuznetsov, W. I. David and N. P. Brandon, *Energy Policy*, 2008, **36**, 4356–4362.
11 Y. Wang, K. S. Chen, J. Mishler, S. C. Cho and X. C. Adroher, *Appl. Energy*, 2011, **88**, 981–1007.
12 F. Barbir, *PEM fuel cells: theory and practice*, Academic Press, 2013.
13 A. Evans, V. Strezov and T. J. Evans, *Renewable Sustainable Energy Rev.*, 2012, **16**, 4141–4147.
14 A. J. Bard and M. A. Fox, *Acc. Chem. Res.*, 1995, **28**, 141–145.
15 C. Perkins and A. W. Weimer, *Int. J. Hydrogen Energy*, 2004, **29**, 1587–1599.
16 A. Steinfeld, *Int. J. Hydrogen Energy*, 2002, **27**, 611–619.
17 S. Abanades, P. Charvin, G. Flamant and P. Neveu, *Energy*, 2006, **31**, 2805–2822.

18 A. Fujishima and K. Honda, *Bull. Chem. Soc. Jpn.*, 1971, **44**, 1148–1150.
19 A. Fujishima and K. Honda, *Nature*, 1972, **238**, 37.
20 H. Dotan, N. Mathews, T. Hisatomi, M. Grätzel and A. Rothschild, *J. Phys. Chem. Lett.*, 2014, **5**, 3330–3334.
21 J. Keeney, D. H. Weinstein and G. M. Haas, *Nature*, 1975, **253**, 719–720.
22 M. S. Wrighton, D. S. Ginley, P. T. Wolczanski, A. B. Ellis, D. L. Morse and A. Linz, *Proc. Natl. Acad. Sci. U. S. A.*, 1975, **72**, 1518–1522.
23 T. Ohnishi, Y. Nakato and H. Tsubomura, *Bunsen-Ges. Phys. Chem., Ber.*, 1975, **79**, 523–525.
24 A. J. Nozik, *Nature*, 1975, **257**, 383–386.
25 J. G. Mavroides, D. I. Tchernev, J. A. Kafalas and D. F. Kolesar, *Mater. Res. Bull.*, 1975, **10**, 1023–1030.
26 A. Fujishima, K. Kohayakawa and K. Honda, *Bull. Chem. Soc. Jpn.*, 1975, **48**, 1041–1042.
27 T. Watanabe, A. Fujishima and K.-i. Honda, *Bull. Chem. Soc. Jpn.*, 1976, **49**, 355–358.
28 J. G. Mavroides, J. A. Kafalas and D. F. Kolesar, *Appl. Phys. Lett.*, 1976, **28**, 241–243.
29 A. B. Ellis, S. W. Kaiser and M. S. Wrighton, *J. Phys. Chem.*, 1976, **80**, 1325–1328.
30 E. Borgarello, J. Kiwi, E. Pelizzetti, M. Visca and M. Grätzel, *Nature*, 1981, **289**, 158–160.
31 M. S. Wrighton, A. B. Ellis, P. T. Wolczanski, D. L. Morse, H. B. Abrahamson and D. S. Ginley, *J. Am. Chem. Soc.*, 1976, **98**, 2774–2779.
32 H. Yoneyama, *Crit. Rev. Solid State Mater. Sci.*, 1993, **18**, 69–111.
33 T. Bak, J. Nowotny, M. Rekas and C. C. Sorrell, *Int. J. Hydrogen Energy*, 2002, **27**, 991–1022.
34 K. Maeda and K. Domen, *J. Phys. Chem. C*, 2007, **111**, 7851–7861.
35 A. Kudo, *Int. J. Hydrogen Energy*, 2007, **32**, 2673–2678.
36 F. E. Osterloh, *Chem. Mater.*, 2008, **20**, 35–54.
37 A. Kudo and Y. Miseki, *Chem. Soc. Rev.*, 2009, **38**, 253–278.
38 K. Maeda and K. Domen, *J. Phys. Chem. Lett.*, 2010, **1**, 2655–2661.
39 X. B. Chen, S. H. Shen, L. J. Guo and S. S. Mao, *Chem. Rev.*, 2010, **110**, 6503–6570.
40 F. E. Osterloh, *Chem. Soc. Rev.*, 2013, **42**, 2294–2320.
41 H. Yoneyama, H. Sakamoto and H. Tamura, *Electrochim. Acta*, 1975, **20**, 341–345.
42 A. J. Nozik, *Appl. Phys. Lett.*, 1976, **29**, 150–153.
43 K. Ohashi, J. McCann and J. O. M. Bockris, *Nature*, 1977, **266**, 610.
44 P. A. Kohl, S. N. Frank and A. J. Bard, *J. Electrochem. Soc.*, 1977, **124**, 225–229.
45 H. Gerischer, *J. Electroanal. Chem. Interfacial Electrochem.*, 1977, **82**, 133–143.
46 R. C. Kainthla, B. Zelenay and J. O. M. Bockris, *J. Electrochem. Soc.*, 1987, **134**, 841–845.
47 A. J. Appleby, A. E. Delahoy, S. C. Gau, O. J. Murphy, M. Kapur and J. O. M. Bockris, *Energy*, 1985, **10**, 871–876.
48 Y. Sakai, S. Sugahara, M. Matsumura, Y. Nakato and H. Tsubomura, *Can. J. Chem.*, 1988, **66**, 1853–1856.
49 N. A. Kelly and T. L. Gibson, *Int. J. Hydrogen Energy*, 2006, **31**, 1658–1673.
50 O. Khaselev, A. Bansal and J. A. Turner, *Int. J. Hydrogen Energy*, 2001, **26**, 127–132.
51 O. Khaselev and J. A. Turner, *Science*, 1998, **280**, 425–427.
52 S. Licht, B. Wang, S. Mukerji, T. Soga, M. Umeno and H. Tributsch, *J. Phys. Chem. B*, 2000, **104**, 8920.
53 A. E. Delahoy, S. C. Gau, O. J. Murphy, M. Kapur and J. O. M. Bockris, *Int. J. Hydrogen Energy*, 1985, **10**, 113–116.
54 G. H. Lin, M. Kapur, R. C. Kainthla and J. O. M. Bockris, *Appl. Phys. Lett.*, 1989, **55**, 386–387.
55 C. Gramaccioni, A. Selvaggi and F. Galluzzi, *Electrochim. Acta*, 1993, **38**, 111–113.
56 R. E. Rocheleau, E. L. Miller and A. Misra, *Energy Fuels*, 1998, **12**, 3–10.
57 S. Y. Reece, J. A. Hamel, K. Sung, T. D. Jarvi, A. J. Esswein, J. J. H. Pijpers and D. G. Nocera, *Science*, 2011, **334**, 645–648.
58 J. Brillet, J.-H. Yum, M. Cornuz, T. Hisatomi, R. Solarska, J. Augustynski, M. Grätzel and K. Sivula, *Nat. Photonics*, 2012, **6**, 824–828.
59 F. F. Abdi, L. Han, A. H. M. Smets, M. Zeman, B. Dam and R. van de Krol, *Nat. Commun.*, 2013, **4**, 2195.
60 L. Han, F. F. Abdi, R. van de Krol, R. Liu, Z. Huang, H. J. Lewerenz, B. Dam, M. Zeman and A. H. Smets, *ChemSusChem*, 2014, **7**, 2832–2838.
61 K. Fujii, S. Nakamura, M. Sugiyama, K. Watanabe, B. Bagheri and Y. Nakano, *Int. J. Hydrogen Energy*, 2013, **38**, 14424–14432.
62 T. J. Jacobsson, V. Fjallstrom, M. Sahlberg, M. Edoff and T. Edvinsson, *Energy Environ. Sci.*, 2013, **6**, 3676–3683.
63 J. Luo, J.-H. Im, M. T. Mayer, M. Schreier, M. K. Nazeeruddin, N.-G. Park, S. D. Tilley, H. J. Fan and M. Grätzel, *Science*, 2014, **345**, 1593–1596.
64 C. R. Cox, J. Z. Lee, D. G. Nocera and T. Buonassisi, *Proc. Natl. Acad. Sci. U. S. A.*, 2014, **111**, 14057–14061.
65 S. W. Boettcher, E. L. Warren, M. C. Putnam, E. A. Santori, D. Turner-Evans, M. D. Kelzenberg, M. G. Walter, J. R. McKone, B. S. Brunschwig, H. A. Atwater and N. S. Lewis, *J. Am. Chem. Soc.*, 2011, **133**, 1216–1219.
66 M. D. Kelzenberg, S. W. Boettcher, J. A. Petykiewicz, D. B. Turner-Evans, M. C. Putnam, E. L. Warren, J. M. Spurgeon, R. M. Briggs, N. S. Lewis and H. A. Atwater, *Nat. Mater.*, 2010, **9**, 239–244.
67 C. Liu, J. Tang, H. M. Chen, B. Liu and P. Yang, *Nano Lett.*, 2013, **13**, 2989–2992.
68 M. R. Shaner, K. T. Fountaine, S. Ardo, R. H. Coridan, H. A. Atwater and N. S. Lewis, *Energy Environ. Sci.*, 2014, **7**, 779–790.
69 B. Liu, C. H. Wu, J. W. Miao and P. D. Yang, *ACS Nano*, 2014, **8**, 11739–11744.
70 A. C. Nielander, M. R. Shaner, K. M. Papadantonakis, S. A. Francis and N. S. Lewis, *Energy Environ. Sci.*, 2015, **8**, 16–25.
71 Z. Chen, T. F. Jaramillo, T. G. Deutsch, A. Kleiman-Shwarsctein, A. J. Forman, N. Gaillard, R. Garland,

K. Takanabe, C. Heske, M. Sunkara, E. W. McFarland, K. Domen, E. L. Miller, J. A. Turner and H. N. Dinh, *J. Mater. Res.*, 2010, **25**, 3–16.
72 B. Parkinson, *Acc. Chem. Res.*, 1984, **17**, 431–437.
73 Z. Chen, H. Dinh and E. Miller, *Photoelectrochemical Water Splitting*, Springer, 2013.
74 M. A. Green, K. Emery, Y. Hishikawa, W. Warta and E. D. Dunlop, *Prog. Photovoltaics*, 2014, **22**, 701–710.
75 K. A. Emery, in *Handbook of Photovoltaic Science and Engineering*, ed. A. Luque and S. Hegedus, John Wiley & Sons, Sussex, 2011, ch. 18, pp. 797–840.
76 http://www.nrel.gov/ncpv/images/efficiency_chart.jpg.
77 P. Bornoz, F. F. Abdi, S. D. Tilley, B. Dam, R. van de Krol, M. Grätzel and K. Sivula, *J. Phys. Chem. C*, 2014, **118**, 16959–16966.
78 X. Wang, K.-Q. Peng, Y. Hu, F.-Q. Zhang, B. Hu, L. Li, M. Wang, X.-M. Meng and S.-T. Lee, *Nano Lett.*, 2014, **14**, 18–23.
79 C.-Y. Lin, Y.-H. Lai, D. Mersch and E. Reisner, *Chem. Sci.*, 2012, **3**, 3482–3487.
80 J. H. Park and A. J. Bard, *Electrochem. Solid-State Lett.*, 2006, **9**, E5–E8.
81 Y. Nakato, N. Takamori and H. Tsubomura, *Nature*, 1982, **295**, 312–313.
82 H. Mettee, J. W. Otvos and M. Calvin, *Sol. Energy Mater.*, 1981, **4**, 443–453.
83 H. Morisaki, T. Watanabe, M. Iwase and K. Yazawa, *Appl. Phys. Lett.*, 1976, **29**, 338–340.
84 G. Peharz, F. Dimroth and U. Wittstadt, *Int. J. Hydrogen Energy*, 2007, **32**, 3248–3252.
85 K. Walczak, Y. Chen, C. Karp, J. W. Beeman, M. Shaner, J. Spurgeon, I. D. Sharp, X. Amashukeli, W. West, J. Jin, N. S. Lewis and C. Xiang, *ChemSusChem*, 2015, **8**, 544–551.
86 N. Gaillard, Y. Chang, J. Kaneshiro, A. Deangelis and E. L. Miller, *Proc. SPIE*, 2010, **7770**, 1–14.
87 F. Zhu, J. Hu, I. Matulionis, T. Deutsch, N. Gaillard, A. Kunrath, E. Miller and A. Madan, *Philos. Mag.*, 2009, **89**, 2723–2739.
88 J. Brillet, M. Cornuz, F. Le Formal, J.-H. Yum and M. Grätzel, *J. Mater. Res.*, 2010, **25**, 17.
89 E. L. Miller, D. Paluselli, B. Marsen and R. E. Rocheleau, *Sol. Energy Mater. Sol. Cells*, 2005, **88**, 131–144.
90 M. A. Modestino, K. A. Walczak, A. Berger, C. M. Evans, S. Haussener, C. Koval, J. S. Newman, J. W. Ager and R. A. Segalman, *Energy Environ. Sci.*, 2014, **7**, 297–301.
91 S. Yamane, N. Kato, S. Kojima, A. Imanishi, S. Ogawa, N. Yoshida, S. Nonomura and Y. Nakato, *J. Phys. Chem. C*, 2009, **113**, 14575–14581.
92 J. H. Park and A. J. Bard, *Electrochem. Solid-State Lett.*, 2005, **8**, G371–G375.
93 Y. Yamada, N. Matsuki, T. Ohmori, H. Mametsuka, M. Kondo, A. Matsuda and E. Suzuki, *Int. J. Hydrogen Energy*, 2003, **28**, 1167–1169.
94 J. R. Bolton, S. J. Strickler and J. S. Connolly, *Nature*, 1985, **316**, 495–500.
95 M. Weber and M. Dignam, *Int. J. Hydrogen Energy*, 1986, **11**, 225–232.
96 S. Licht, *J. Phys. Chem. B*, 2001, **105**, 6281–6294.
97 S. Haussener, C. X. Xiang, J. M. Spurgeon, S. Ardo, N. S. Lewis and A. Z. Weber, *Energy Environ. Sci.*, 2012, **5**, 9922–9935.
98 S. Haussener, S. Hu, C. Xiang, A. Z. Weber and N. S. Lewis, *Energy Environ. Sci.*, 2013, **6**, 3605–3818.
99 H. Doscher, J. F. Geisz, T. G. Deutsch and J. A. Turner, *Energy Environ. Sci.*, 2014, **7**, 2951–2956.
100 S. Hu, C. X. Xiang, S. Haussener, A. D. Berger and N. S. Lewis, *Energy Environ. Sci.*, 2013, **6**, 2984–2993.
101 K. Fujii, S. Nakamura, K. Watanabe, B. Bagheri, M. Sugiyama and Y. Nakano, *MRS Proc.*, 2013, 1491.
102 B. M. Kayes, H. Nie, R. Twist, S. G. Spruytte, F. Reinhardt, I. C. Kizilyalli and G. S. Higashi, 2011 37th IEEE Photovoltaic Specialists Conference, IEEE, 2011, pp. 000004–000008, DOI: 10.1109/PVSC.2011.6185831.
103 W. Shockley and H. J. Queisser, *J. Appl. Phys.*, 1961, **32**, 510–519.
104 B. D. James, G. N. Baum, J. Perez, K. N. Baum and O. V. Square, Directed Technologies Inc., Department of Energy contract GS-10F-009J technical report, 2009.
105 B. A. Pinaud, J. D. Benck, L. C. Seitz, A. J. Forman, Z. B. Chen, T. G. Deutsch, B. D. James, K. N. Baum, G. N. Baum, S. Ardo, H. L. Wang, E. Miller and T. F. Jaramillo, *Energy Environ. Sci.*, 2013, **6**, 1983–2002.
106 P. Zhai, S. Haussener, J. Ager, R. Sathre, K. Walczak, J. Greenblatt and T. McKone, *Energy Environ. Sci.*, 2013, **6**, 2380–2389.
107 R. Sathre, C. D. Scown, W. R. Morrow, J. C. Stevens, I. D. Sharp, J. W. Ager, K. Walczak, F. A. Houle and J. B. Greenblatt, *Energy Environ. Sci.*, 2014, **7**, 3264–3278.
108 S. Y. Chen and L. W. Wang, *Chem. Mater.*, 2012, **24**, 3659–3666.
109 R. Liu, Z. Zheng, J. Spurgeon and X. G. Yang, *Energy Environ. Sci.*, 2014, **7**, 2504–2517.
110 C. A. Rodriguez, M. A. Modestino, D. Psaltis and C. Moser, *Energy Environ. Sci.*, 2014, **7**, 3828–3835.
111 Department of Energy, Fuel Cell Technologies Office Multi-Year Research, Development and Demonstration Plan, http://energy.gov/eere/fuelcells/fuel-cell-technologies-office.

